Formation Characteristics of the Commensurate Fluorite-Type $Bi_2O_3-Nb_2O_5$ Solid Solution

Urša Pirnat,* Matjaz Valant, Boštjan Jančar, and Danilo Suvorov

Jožef Stefan Institute, Jamova 39, SI-1000 Ljubljana, Slovenia

Received April 28, 2005. Revised Manuscript Received August 4, 2005

X-ray powder diffraction and transmission electron microscopy were used to investigate the formation characteristics and stability range of the tetragonal modification of a fluorite-type $Bi_2O_3-Nb_2O_5$ solid solution. The results showed that this tetragonal, commensurately modulated phase forms through the intermediate formation of the incommensurately modulated cubic fluorite phase followed by the incommensurate−commensurate transformation. This transformation can be described as a homogeneous nucleation with a temperature-dependent induction time and growth kinetics, which is determined by a growth rate of the tetragonal domains nucleated during the induction time. The homogeneity range of the tetragonal phase was found to extend between $-0.2 \le y \le 0.04$ for the general formula $Bi_{3-y}Nb_{1+y}O_{7+y}$. The tetragonal $Bi_{3-y}Nb_{1+y}O_{7+y}$ phase is thermally stable up to the transition temperature where it transforms back to the cubic incommensurate phase. The transition temperature increases with Nb concentration from 750 °C for $y = -0.2$ to 920 °C for $y = 0.04$.

Introduction

The high-temperature δ-Bi_2O_3 form is stable from the transition temperature ($\alpha \rightarrow \delta$) at 729 °C up to the melting point at 825 °C.[1] δ-Bi_2O_3 crystallizes in a face-centered cubic (fcc) crystal structure, akin to the defect fluorite-type unit cell,[2] and exhibits several unique features: a high polarizability of the cation network, the ability of bismuth cations to dynamically accommodate asymmetric surroundings,[3] and, most importantly, the anion network containing 25% of the intrinsic vacancies ($BiO_{1.5/0.5}$ = oxygen vacancy) as a result of the stoichiometry of the unit cell. Because of the highly disordered defect fluorite structure of δ-Bi_2O_3 an interstitial vacancy transport of the oxygen ions leads to an exceptionally high oxide ion conductivity.[4] To maintain the δ-Bi_2O_3 crystal structure and its ion-conducting properties below the $\alpha \rightarrow \delta$ transition temperature at 729 °C, a stabilization using Bi substitution with different metal cations was performed.[5−12] In this way a variety of Bi_2O_3-rich fcc fluorite solid solutions were stabilized at room temperature.[5−12] A very large family of the fluorite-type oxygen ion conducting solid solutions based on δ-Bi_2O_3 have been investigated as promising materials for solid oxide fuel cells, electrochemical sensors, dual-phase membranes, and catalysts.[5−13] To understand the mechanism of the ionic transport, many studies were performed, and they showed some common features,[5−13] for example, that the ionic conductivity of δ-Bi_2O_3 solid solutions increases with a decrease in the dopant concentration and the efficiency of the stabilization of the fcc form depends on the ionic radius of the dopants.[3,8]

Among the large choice of cations that can be used for the stabilization of the δ-Bi_2O_3 structure, Nb is one of the most frequently used. The $(Bi_2O_3)_{1-x}-(Nb_2O_5)_x$ solid solutions (hereafter δ-BN_{SS}) that form in the compositional range $0.1 \ge x \ge 0.26$ exhibit one of the highest ionic conductivities among Bi_2O_3-based fluorites.[10−12] A maximum in the conductivity is observed at the lower limit of the substituent concentration that still stabilizes the δ-Bi_2O_3 structure. The structure was determined as $3 + 3D$ incommensurately modulated, with an underlying average fluorite unit cell that has the space-group symmetry $Fm3m$.[14] The compositional and displacive perturbation are determined in three dimensions of the fluorite-related substructure, and the modulation parameter has a value of $\epsilon \sim 0.37$ for the $x = 0.25$ composition. The structure is based on corner-shared chains of NbO_6 octahedra along the $\langle 110 \rangle_F$ direction of the fcc subcell, and it is known in the literature as type II.

In addition to the most frequently considered use of δ-BN_{SS} as a solid electrolyte, recently they were also suggested for use in low-temperature co-fired ceramic

* To whom correspondence should be addressed. E-mail address: ursa.pirnat@ijs.si.

(1) Roth, R. S.; Waring, J. L. *J. Res. Natl. Bur. Stand. (U.S.)* **1962**, *66A*, 451.
(2) Harwig, H. A. *Z. Anorg. Alleg. Chem.* **1978**, *444*, 151.
(3) Boivin, J. C.; Mairese, G. *Chem. Mater.* **1998**, *10*, 2870.
(4) Depero, L. E.; Sangaletti, L. *J. Solid State Chem.* **1996**, *122*, 439.
(5) Iwahara, H.; Esaka, T.; Sato, T.; Takahashi, T. *J. Solid State Chem.* **1981**, *39*, 173.
(6) Esmaeilzadeh, S.; Lundgren, S.; Halenius, U.; Grins, J. *J. Solid State Chem.* **2000**, *156*, 168.
(7) Takahashi, T.; Esaka, T.; Iwahara, H. *J. Solid State Chem.* **1976**, *16*, 317−323.
(8) Kharton, V. V.; Naumovich, E. N.; Yaremchenko, A. A.; Marques, F. M. B. *J Solid State Electrochem.* **2001**, *5*, 160.
(9) Fung, K. Z.; Virkar, A. V. *J. Am Ceram. Soc.* **1991**, *74*, 1970.
(10) Takahashi, T.; Iwahara, H.; Esaka, T. *J. Electrochem. Soc.* **1977**, *124*, 1563.
(11) Takahashi, T.; Iwahara, H. *Mater. Res. Bull.* **1978**, *13*, 1447.
(12) Yaremchenko, A. A.; Kharton, V. V.; Naumovich, E. N.; Vecher, A. A. *J. Solid State Electrochem.* **1998**, *2*, 146.
(13) Boyapati, S.; Wachsman, E. D.; Jiang N. *Solid State Ionics* **2001**, *140*, 149.
(14) Withers, R. L.; Ling, C. D.; Schmid, S. *Z. Kristallogr.* **1999**, *214*, 296.

10.1021/cm0509025 CCC: $30.25
Published on Web 09/02/2005

technology as a high-permittivity glass-free dielectric layer.[15] An unusual scattering of dielectric properties as a function of processing temperature was observed for the $x = 0.25$ composition and was attributed to the formation of another structural modification.[16] The structural model proposed for this modification is the tetragonal fluorite-based unit cell with a $I\bar{4}m2$ space group.[17] In contrast to the cubic modification, the tetragonal modification is described as an ordered $3 \times 3 \times 7$ superstructure of the fluorite-type δ-Bi_2O_3. This phase uses the same motif of $\langle 110 \rangle_F$ strings of NbO_6 octahedra to preserve the fluorite-type substructure, but in contrast to the type II, the symmetry is lowered because of the compromised and strained $\langle 110 \rangle_F$ strings, and it can be described as a hybrid of the fluorite and pyrochlore structural types. The type III phase, as the tetragonal modification is also called, is according to Ling et al.[17,18] thermodynamically stable from room temperature up to the melting point at 1100 °C and was in the $Bi_2O_3-Nb_2O_5$ phase diagram described as a discrete phase with the composition $x = 0.25$.[17,18] The type III phase is the most Nb-rich phase in this system, and it has the fluorite-related underlying subcell.

The literature descriptions of the phase relations in the Bi_2O_3-rich part of the $Bi_2O_3-Nb_2O_5$ system differ significantly. The first existence of the tetragonal form was reported by Zhou and Jefferson[19] for $x = 0.30$. In contrast to the early studies, in which two cubic fluorite analogues were suggested,[1] Zhou et al.[19] proposed four superstructural varieties of the $Bi_2O_3-Nb_2O_5$ fluorite-based solid solutions by use of electron diffraction. In addition, later studies claimed the coexistence of the type II and type III within the compositional range from $x = 0.23$ to 0.25.[18] For the end member of the two-phase region the literature is again inconsistent. Castro et al.[20] synthesized a single crystal of the cubic type II structure by cooling the melted $x = 0.25$ composition from 1100 °C, while Ling et al.[18] reported for the same composition the formation of the single-phase type III at 900 °C.

Our initial investigations indicated that the incommensurate, cubic type II phase undergoes a phase transition to the commensurate, tetragonal type III phase.[21] In the same study we showed that the ion ordering of these materials has a profound influence on the dielectric properties and conductivity, which are both technologically highly important properties. We have also seen that the kinetics of the transition strongly depends on the processing conditions. Although the crystal structure is already resolved, the conditions for the tetragonal-phase formation have never been determined. Therefore, in the present study we investigated the kinetics aspects of the tetragonal-phase formation. In addition, we determined the processing conditions together with the temperature and the compositional stability of the tetragonal phase, which allows us to define the phase relations in this part of the phase diagram. Understanding these parameters is very important for the controlled and reproducible synthesis of the tetragonal modification, the optimization of its electrical properties, and the utilization of this compound in the electronic industry.

Experimental Procedures

The nominal amounts of reagent-grade oxides (Bi_2O_3, 99.975%, Alfa Aesar, and Nb_2O_5, 99.9+%, Alfa Aesar), corresponding to the general formula $(1 - x)Bi_2O_3-xNb_2O_5$, were homogenized in a mortar with acetone. To study the solid-state reactions that occur at a particular temperature a mixture of oxides with the nominal composition $x = 0.25$ was quenched in air to room temperature after each firing. For the studies of the kinetics of the tetragonal-phase formation the powders were first preheated at 700 °C for 10 h, ground, and reheated at 700 °C for 5 h. The ground-and-milled powders were then unaxially pressed (at ~150 MPa) into pellets with a diameter of 6 mm and a height of 3 mm. The pellets were then annealed in air for different times under isothermal conditions at 800, 820, 840, 860, and 880 °C. For the studies of the phase relations we prepared mixtures with nominal compositions in the range of $0.18 < x < 0.30$ using the same calcination procedure as for the kinetic studies. To ensure accurate heat treatments the furnaces were repeatedly calibrated with an external Pt−Rh thermocouple.

The X-ray powder diffraction (XRD) analysis was performed with a Bruker AXS D4 Endeavor diffractometer using Cu Kα radiation. The data were collected in the range $2 < 2\theta < 90°$ with a step of 0.02°, a counting time of 4 s, and variable V12 slits. All of the XRD patterns were collected at room temperature.

To evaluate the extent of the phase transformation a quantitative analysis of the volume fraction of the phases present was performed by determining the integrated peak intensities, using the DIFFRAC^{plus} EVA, version 8.0, program (Bruker AXS). The volume fraction of the formed tetragonal phase, $X(t)$, at time t was calculated from the X-ray diffraction pattern using the equation:

$$X(t) = \frac{I_{hkl}^{T1} + I_{hkl}^{T2}}{I_{hkl}^{T1} + I_{hkl}^{T2} + I_{hkl}^{C}} \quad (1)$$

where I_{hkl}^{T1}, I_{hkl}^{T2}, and I_{hkl}^{C} denote the integrals of the tetragonal and cubic reflections, respectively. For the quantitative phase analysis we focused on the cubic reflections [311], [222], and [422] and their tetragonal analogues,[9] for which no overlapping was noticed. The average of the quantitative analyses performed on these three diffraction ranges was used as a result.

The DIFFRAC^{plus} Topas R program (Bruker AXS) was used for the determination of the lattice parameters of the $Bi_{3-y}Nb_{1+y}O_{7+y}$, $0.04 \geq y \geq -0.02$ solid solution with a Rietveld refinment of the XRD data.

A JEOL 4000FX transmission electron microscope (TEM) equipped with a Gatan heating stage, operating up to 1000 °C, was used to perform an in situ study of the phase transformation. The temperature control in such a heating stage is achieved with a system composed of a Pt−Pt 13% Rh thermocouple and a current-regulating mechanism which, according to the specification, ensures changes of less than 0.0001 °C during the 5 s of exposure. For the TEM study the electron-transparent thin foils were prepared by mechanical thinning of the sintered samples followed by ion milling using argon ions at 3.5 kV.

(15) Valant, M.; Suvorov, D. *Bol. Soc. Esp. Ceram. Vidrio* **2004**, *43*, 634.
(16) Valant, M.; Suvorov, D. *J. Am. Ceram. Soc.* **2003**, *86*, 939.
(17) Ling, C. D.; Johnson, M. *J. Solid State Chem.* **2004**, *177*, 1838.
(18) Ling, C. D.; Withers, R. L.; Schmid, S.; Thompson, J. G. *J. Solid State Chem.* **1998**, *137*, 42.
(19) Zhou, W.; Jefferson, D. A. *Proc. R. Soc. London, Ser. A* **1986**, *406*, 173.
(20) Castro, A.; Aguado, E.; Rojo, J. M.; Herrero, P.; Enjalbert, R.; Galy, J. *Mater. Res. Bull.* **1998**, *33*, 31.
(21) Valant, M.; Jančar, B.; Pirnat, U.; Suvorov, D. *J. Eur. Ceram. Soc.* **2005**, *25*, 2829.

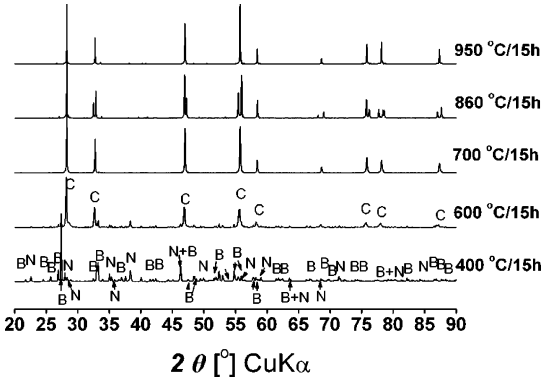

Figure 1. X-ray diffraction pattern of the reaction mixture with a nominal composition of $x = 0.25$ after firing for 15 h at different temperatures (B = Bi_2O_3, N = Nb_2O_5).

Results and Discussion

Synthesis and Reaction Mechanism. The X-ray patterns of the mixture with 25 mol % of Nb_2O_5 after annealing for 15 h at different temperatures ranging from 400 to 950 °C are presented in Figure 1. Sets of the most intensive peaks on the X-ray pattern of the sample quenched from 400 °C belong to the starting oxides: Bi_2O_3 and Nb_2O_5. These peaks are reduced in intensity after further heat treatment at 500 °C, and new peaks appear, which could be ascribed to the formation of the type II phase. On the basis of this result we concluded that initially the cubic incommensurate phase is formed directly from the reaction mixture in the temperature range from 400 to 600 °C. No evidence for the formation of intermediate phases was found. At a temperature of 700 °C we obtained the single-phase cubic type II phase. However, an X-ray pattern of the same sample fired at 860 °C differed significantly from that obtained after firing at 700 °C. A comparison revealed that the main peaks appeared at approximately the same angles but exhibited a tetragonal splitting typical for the type III phase.[16] At a higher temperature (950 °C) the type III phase again transformed into the cubic type II phase, which is not in accordance with the literature claims about the tetragonal phase being stable up to the melting point at 1110 °C.[18] A detailed comparison of the two X-ray patterns of the type II phase, obtained at 700 and 950 °C (Figure 2), reveals the structural identity on the level of the prototype cell and the incommensurate modulation.[14] Because of this unusual phase-transition sequence, from cubic-incommensurate to tetragonal-commensurate and back to the same cubic-incommensurate phase, further detailed investigations of the thermodynamics and kinetics of the phase transformation were undertaken.

Kinetics of the Phase Transformation. The studies of the kinetics of the phase transformation from the cubic-to-tetragonal modification were performed on the sample with the $x = 0.25$ composition, which was pre-reacted at 700 °C to obtain a pure cubic type II phase. Figure 3 represents the formation of the tetragonal phase from the cubic as a function of annealing time at a temperature of 860 °C. The formation of the tetragonal phase is evident from a series of tetragonal reflections, which appears on both sides of the cubic [311] reflections. The transformation to the tetragonal modification proceeded with time until after 9 h the cubic phase completely disappeared.

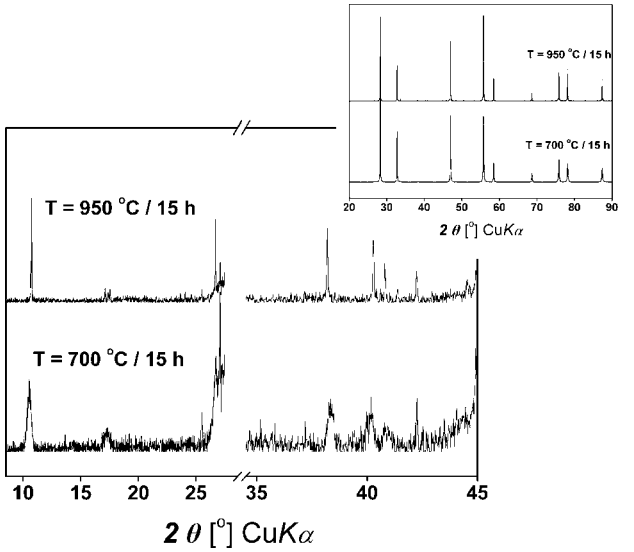

Figure 2. Comparison of X-ray patterns of the cubic type II phase obtained directly from the starting mixture by firing at 700 °C/15 h and the type II phase obtained with the transformation from the tetragonal type III phase at 950 °C.

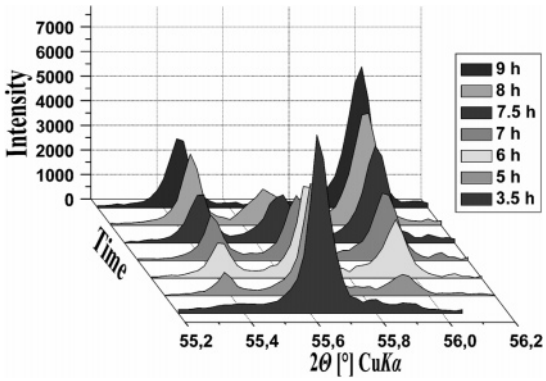

Figure 3. Formation of the tetragonal phase as a function of annealing time at 860 °C. Only the range of diffraction angles around the [311] reflection of the type II is shown.

The volume fraction $X(t)$, calculated from XRD measurements as described in the experimental section, as a function of annealing time and temperature for the $x = 0.25$ composition is presented in Figure 4. The point-to-point curves are drawn through the experimental data for the isothermal formation of the tetragonal phase at temperatures of 800, 820, 840, 860, and 880 °C and represent a characteristic time scale for the formation of the tetragonal phase at a particular temperature.

From the kinetic curves in Figure 4 we can see that the process of the transformation involves two distinct steps. Through the initial period of time, the so-called induction time, no macroscopic changes in the phase composition can be observed. The induction time is followed by a period when the course of the transformation to the tetragonal phase can be monitored by X-ray diffraction.

The experimental data show that the induction time significantly varies with the annealing temperatures. At 800 °C the induction time is 10 h, and this time decreases with an increase in the annealing temperature. At 820, 840, 860, and 880 °C the induction times decrease to 4.75, 4, 2.4, and 2.1 h, respectively. The general behavior of the induction time corresponds well with the description of the transforma-

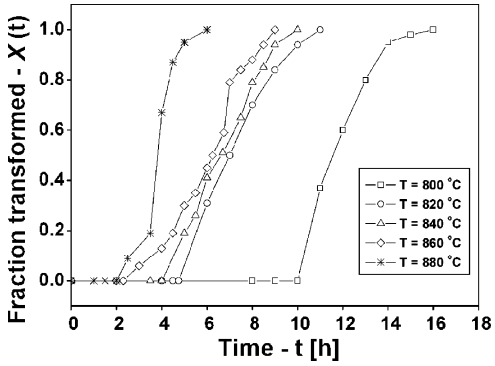

Figure 4. Fraction of the tetragonal modification of the $Bi_2O_3-Nb_2O_5$ fluorite solid solution with the $x = 0.25$ composition as a function of the annealing time and temperature.

tions as a homogeneous nucleation. The induction time (τ) for such a type of transformation was described as[22]

$$\tau \cong \frac{6d^2n^*}{D \ln S} \tag{2}$$

where d stands for the diameter of the diffusing particle, n^* stands for the critical number of the particles in the critical nucleus, D is the diffusion coefficient, and S is the supersaturation. The supersaturation in our case is proportional to the difference between the annealing temperature (T_{ann}) and the transformation temperature from the tetragonal back to the cubic modification (T_{tc}). A higher supersaturation exists at lower temperatures, and S decreases linearly with increasing T_{ann}. The Arrhenius relationship describes the opposite trend for the temperature dependence of D: $\ln(D)$ increases in proportion to $1/T_{ann}$. Because in eq 2 the increase in D strongly dominates over the decrease in $\ln(S)$, the induction time must decrease with T_{ann}, and this is exactly what our experiments have shown. The behavior of the induction time as a function of annealing temperature demonstrates that the observed transformation is close to homogeneous nucleation. According to this, during the induction stage the species organize themselves in ordered nuclei, which try to grow above the critical size. This process is thermodynamically driven, but its kinetics is mainly governed by the diffusivity of the species. The consequence of this is that a sufficiently high annealing temperature is required to overcome the induction time in an experimentally reasonable time. For instance, at an annealing temperature of 700 °C no tetragonal phase was formed, even after 100 h.

In the second stage of the transformation, as the tetragonal phase starts to appear, the kinetic curves develop a sigmoid shape typical of a transformation based on nucleation and domain growth during a solid-state phase transition. In this stage the total rate of the phase transition depends not only on the growth of domains from the stable nuclei formed during the induction time but also on the formation of new, stable nuclei and their growth. The expression used to interpret the experimental data was developed by Avrami.[23]

$$X(t) = 1 - \exp(-kt^n) \tag{3}$$

Using a fitting procedure for the experimental data from Figure 4 we calculated the Avrami exponent n, which describes the mechanism that determines the kinetics of the transformation, and the rate constant k, which describes the rate of the transformation. The calculations showed that the Avrami exponent n has a value of 1.5 ± 0.2. According to Rao and Rao,[24] this indicates that the kinetics of this stage is governed by the growth of domains nucleated during the induction time, whereas the formation of new, stable nuclei and their growth has a negligible contribution. In addition, we noticed that n shows a slight temperature dependency and increases from 1.4 to 1.7 for isothermal treatments at 800 °C and 880 °C. This deviation from theory can be ascribed to the fact that the temperature has a slight influence on the growth mechanism, especially in the case of a diffusion-controlled transition.[23,24]

The rate constant k, calculated from the experimental data, is of the same order of magnitude (10^{-7} s^{-1}) for the whole temperature interval investigated. The approximately constant transformation rate can also be estimated from the steepness of the transition curves in Figure 4.

This means that the cubic-to-tetragonal transformation of the $Bi_2O_3-Nb_2O_5$ fluorite solid solution, which is an incommensurate−commensurate transformation that involves a cation ordering,[21] can be described as a homogeneous nucleation with a temperature-dependent induction time. In addition, the kinetics of the transition is dominated by the growth rate of tetragonal domains nucleated during the induction time.

The existence of an induction time required for the formation of a stable nucleus and its subsequent growth was confirmed by the in situ high-temperature experiment performed in the TEM. The bright-field imaging and the selected-area electron diffraction were used to track the changes within a cubic-phase grain during an annealing at 880 °C. During the first 2.5 h no changes were observed either in the morphology of the grain or its crystal-structure modulation. After that time, however, an inclusion appeared within the cubic grain. Upon further annealing at the same temperature the inclusion started to grow, as shown in Figure 5.

From the experimental data regarding the cubic-to-tetragonal transformation kinetics, obtained for the solid solution with $x = 0.25$, we constructed a temperature−time diagram (Figure 6). The bottom curve in the diagram indicates the induction time at different temperatures, whereas the upper curve represents the time needed for a complete transformation to the tetragonal phase. Furthermore, a straight horizontal line at $T = 900$ °C represents the high-temperature limit for obtaining the tetragonal phase, above which the transformation back to the incommensurate cubic phase occurs. With respect to the phase composition the diagram, thus, divides the temperature−time domain of the $x = 0.25$ solid solution into four regions. The cubic phase is obtained either by firing above 900 °C or by applying a

(22) Ring, T. A. *Fundamentals of Ceramic Powder Processing and Synthesis*; Academic Press, Inc.: San Diego, 1979.
(23) Avrami, M. *J. Chem. Phys.* **1939**, *7*, 1103.
(24) Rao, C. N. R.; Rao, K. J. *Phase Transitions in Solids*; McGraw-Hill: New York, 1978.

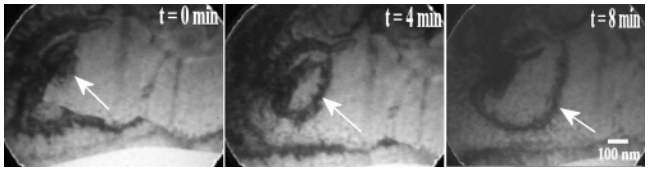

Figure 5. In situ TEM bright-field images of the growth of an inclusion. The arrows show the domain of the tetragonal commensurate phase, which is growing from the cubic incommensurate matrix at $T = 880$ °C, starting after an induction time of $\tau_0 = 2.5$ h.

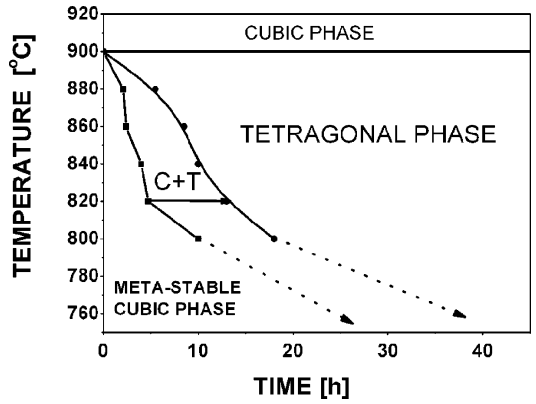

Figure 6. Temperature−time diagram for the formation of cubic and tetragonal fluorite-based $(1 - x)Bi_2O_3$−xNb_2O_5 modifications with $x = 0.25$.

combination of firing time and temperature that falls in the region under the lower curve of the diagram. Between the two curves is the region of incomplete phase transformation, representing firing times and temperatures that yield a mixture of cubic and tetragonal phases. Above the upper curve but below the straight line is the region of the tetragonal phase.

The temperature−time diagram indicates that the commensurately ordered tetragonal phase of the solid solution with $x = 0.25$ is a thermodynamically stable phase at temperatures below 900 °C. Its formation, however, proceeds via the formation of the incommensurate cubic phase, followed by a phase transformation. This cubic-to-tetragonal phase transformation seems to be relatively slow, and except for the close proximity of the high-temperature stability limit of the tetragonal phase, it takes, because of the long induction times, several hours or even days to complete. At temperatures below 700 °C the induction time exceeds 100 h.

Thermal Stability and Phase Equlibria. Further experiments revealed that the commensurately modulated tetragonal phase (type III) can also be obtained for compositions with x other than 0.25. By annealing at temperatures between 700 and 950 °C we synthesized single-phase type III compounds for several compositions in the range $x = 0.20$−0.26. From Figure 7 it is clear that the volume of the unit cell of the tetragonal phase gradually decreases as x increases toward 0.26. As x exceeds 0.26 the $Bi_5Nb_3O_{15}$ phase forms in addition to the commensurate tetragonal solid solution. These results imply the existence of a $Bi_{3-y}Nb_{1+y}O_{7+y}$ homogeneity range of the type III structure, with the upper concentration limit of Nb_2O_5 at $y = 0.04$ and the lower limit stretching at least to $y = -0.2$.

As was the case for the composition with $x = 0.25$, other compositions within the homogeneity range also exhibit the

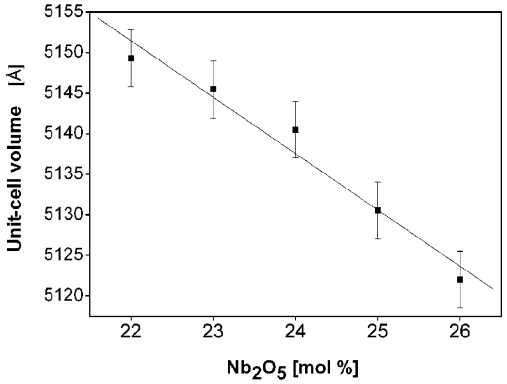

Figure 7. Volume of the tetragonal unit cell as a function of Nb_2O_5 concentration.

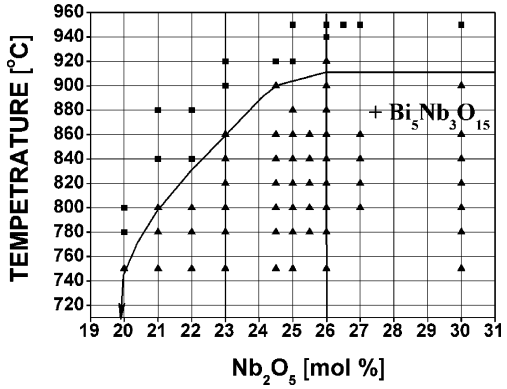

Figure 8. XRD phase analysis results as a function of temperature and concentration (■ is where the cubic phase was detected and ▲ is where the tetragonal phase was detected).

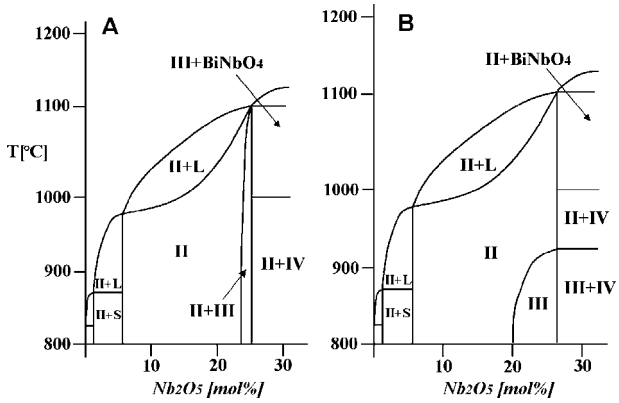

Figure 9. Correction of the Bi_2O_3-rich part of the Bi_2O_3−Nb_2O_5 phase diagram (A, diagram from data of Ling et al.;[18] B, diagram corrected according to the results of this study).

high-temperature stability limit of the commensurate tetragonal phase. Upon heating above this temperature the type III tetragonal phase transforms into the incommensurately modulated type II cubic phase. In contrast to the cubic-to-tetragonal transformation, this occurs almost instantaneously. The high-temperature stability limit of the tetragonal-phase homogeneity range was, therefore, probed by quenching a series of compositions from temperatures up to 950 °C, followed by X-ray diffraction analyses.

The diagram shown in Figure 8 reveals that with an increase in the Nb_2O_5 concentration within the $Bi_{3-y}Nb_{1+y}O_{7+y}$ homogeneity range the temperature of the tetragonal-to-cubic transformation (type III to type II) gradually increases,

implying the higher thermal stability of the type III phase in the case of solid solutions with a higher Nb_2O_5 content. The thermal stability in turn influences the time scale within which the type III phase can be synthesized. Near the upper concentration limit (26 mol % of Nb_2O_5), soaking at a temperature as high as 920 °C can be applied for the synthesis of the type III phase, which according to the trend indicated in Figure 4 significantly reduces the required induction time. At the lower concentration limit, on the other hand, the type III phase is stable below 750 °C, which considerably slows the kinetics of its formation and, thus, severely limits the feasibility of the synthesis.

On the basis of our findings we can conclude that the existence of the type III phase is not limited to a composition with 25 mol % of Nb_2O_5, as previously reported,[17,18] but it is stable across a broader compositional range stretching from 20 to 26 mol % of Nb_2O_5. Furthermore, its thermal stability significantly differs from that described in the literature. Instead of being stable up to the melting point as reported,[18] the type III phase transforms into the incommensurate type II phase at a specific temperature, which varies from 920 °C at 26 mol % of Nb_2O_5 to 750 °C at 20 mol % Nb_2O_5. To account for these new findings the existing $Bi_2O_3-Nb_2O_5$ phase diagram[18] needs to be altered, as shown in Figure 9.

Conclusions

The type III commensurate phase from the $Bi_2O_3-Nb_2O_5$ system is stable within the $Bi_{3-y}Nb_{1+y}O_{7+y}$ homogeneity range ($-0.2 < y < 0.04$). Its stability region is confined by the transition temperature to the cubic incommensurate fluorite phase. The transition temperature increases with Nb concentration from 750 °C for $y = -0.2$ to 920 °C for $y = 0.04$. During the synthesis of the type III solid solutions, however, the incommensurate phase is the first to form, regardless of the reaction temperature. Consequently, the formation of the commensurate phase, within its stability range, proceeds via a phase transformation from its incommensurate counterpart. The transformation occurs in two stages. The first stage is characterized by a temperature-dependent induction time required for the formation of stable nuclei, which implies a mechanism similar to homogeneous nucleation. At temperatures closer to the high-temperature stability limit the induction time is shorter and the transformation kinetics is governed by the growth of domains nucleated during the induction time. The kinetics of the growth was not significantly temperature-dependent in the narrow temperature range investigated.

CM0509025